Eur Biophys J (1987) 15: 237–249

European Biophysics Journal

Low temperature X-ray investigation of structural distributions in myoglobin *

F. Parak [1] **, H. Hartmann [1], K. D. Aumann [1], H. Reuscher [1], G. Rennekamp [1], H. Bartunik [2], and W. Steigemann [3]

[1] Institut für Physikalische Chemie der Universität Münster, Schloßplatz 4–7, D-4400 Münster, Federal Republic of Germany
[2] Max-Planck-Institut, Außenstelle Hamburg, D-2000 Hamburg, Federal Republic of Germany
[3] Max-Planck-Institut für Biochemie, D-8033 Martinsried, Federal Republic of Germany

Received January 9, 1987/Accepted in revised form May 1, 1987

Abstract. The results of X-ray structure analysis of metmyoglobin at 300 K, 185 K, 165 K, 115 K and 80 K are reported. The lattice vectors **a** and **b** decrease linearly with temperature while **c** shows non-linearity above 180 K, indicating some type of phase transition. Cooling does change the myoglobin structure but only within the structural distribution as determined by individual $\langle x^2 \rangle$-values at room temperature. Two residues showed significant alternative positions for side-chains at higher temperatures while only one position is occupied at low temperatures. In the case of LEU 61 a jump between different positions of the side-chain reduces the potential barrier for the entrance of the O_2 molecule to the heme pocket.

The mean square displacements, $\langle x^2 \rangle$, of the individual residues decrease linearly with temperature in most cases, indicating a parabolic envelope for the potential responsible for motions. A separation of rotational and translational disorder of the entire molecule is discussed. Comparison with Mössbauer spectroscopy indicates that protein dynamics on a time scale faster than 10^{-7} s is not simply a harmonic process. Extrapolation of the structural distributions to $T = 0$ K shows that a large zero point distribution of the myoglobin structure exists, thus proving that there is no absolute energy minimum for one well defined conformation.

Key words: Protein crystallography, Debye-Waller factor, intramolecular motion, oxygen path

Introduction

Our knowledge of the three-dimensional architecture of molecules is essentially based on X-ray structure investigations. Even in the case of macromolecules, such as proteins, precise information is obtained on the coordinates of the atoms of the molecules. Besides the structure, data analysis of X-ray experiments yields the temperature factor. It is a measure of the mean-square displacements of the atoms from their average coordinates. In small molecules it is usual to give mean-square displacement tensors for all atoms. In proteins the situation is more complicated. The complexity of the structure makes it desirable to reduce free parameters to a minimum during data analysis. Therefore, for many years it has been general practice to assume that the temperature factor is isotropic and common for all atoms in a molecule. For very large molecules and in the case of low resolution one still uses this restriction.

X-ray structure analysis reveals not only the static conformation of a protein but also protein dynamics. For a detailed analysis it is, however, necessary to give up the simplification of a common temperature factor and to determine the individual mean-square displacements, $\langle x^2 \rangle$, of non-hydrogen atoms in the molecule. Some years ago, a first analysis of this type was performed for lysozyme (Artymiuk et al. 1979) and for myoglobin (Frauenfelder et al. 1979).

The discussion of the individual mean-square displacements answers a number of questions concerning the physical picture of protein dynamics. In the case of lysozyme it was shown that molecules with a similar tertiary structure have similar $\langle x^2 \rangle$-values along their sequence. Such a result has also been obtained in a comparison of myoglobin and erythrocruorin although differences which may be related to functional properties do occur (Hartmann et al. 1986).

Discussing protein dynamics in terms of $\langle x^2 \rangle$-values one has to have in mind that X-ray structure analysis is unable to resolve static and dynamic effects. Measurements are performed on crystals containing typically 10^{15} molecules. At any instant all possible vibrational amplitudes of atoms are present in a crystal with the appropriate weighting factor. If it were possible to stop all motion and freeze atoms in

* Dedicated to Prof. H. Frauenfelder on his 65th birthday
** To whom offprint requests should be sent

position the $\langle x^2 \rangle$-values obtained by X-ray structure analysis would not change. From these considerations it is clear that experimentally obtained $\langle x^2 \rangle$-values do not necessarily reflect motion. A crystal containing 10^{15} rigid protein molecules having a slightly different structure also yields individual $\langle x^2 \rangle$-values. Large mean-square displacements indicate regions in the molecule which have larger differences in structure while vanishingly small $\langle x^2 \rangle$-values indicate regions where all molecules are identical.

In protein molecules, dynamic as well as static structural differences contribute to the mean-square displacements. Thermal vibrations occur as in any other solid. The tertiary structure is determined by relatively weak forces making structural variations probable (compare: Parak et al. 1987a). In order to separate static and dynamic effects the temperature dependence of the $\langle x^2 \rangle$-values can be used. Slow temperature reduction freezes out motions while static disorder is not affected. In the case of myoglobin Frauenfelder et al. (1979) performed structure investigations at 300 K, 275 K and 250 K to examine protein dynamics. Although this paper gave a fundamental insight into protein dynamics, the temperature interval was too small for valid conclusions concerning the temperature dependence of motion. The structure determination at 80 K by Hartmann et al. (1982) improved the situation. It showed, however, that a conclusive discussion has to be based on more measurements.

In this contribution we report X-ray structure investigations of metmyoglobin at 300 K, 185 K, 165 K, 115 K and 80 K. All structures were measured and refined in the same way. The analysis of the $\langle x^2 \rangle$-values has been performed in a consistent way. The results give a large number of new insights into the physical nature of protein dynamics. It becomes, however, obvious that the power of the method is not exhausted by this investigation. Additional structures should be determined in the temperature range below 80 K and between 180 K and 300 K.

Experimental procedure

Crystals of met-Mb were grown according to the method of Kendrew and Parrish (1956). Protein crystals are usually destroyed when they are cooled below the freezing point of their mother liquor. To prevent this, the crystals used for the low temperature experiments were shock frozen according to the method of Parak et al. (1977). The crystals are fixed in a Debye capillary tube by a very small amount of mother liquor. After freezing the connection between the glass and the crystal is rather tight. The capillary is mounted on a goniometer head and oriented so that the *b*-axis becomes approximately the rotation axis. The orientation is not controlled by X-ray photographs. Misalignment is taken into account only in the data evaluation. After freezing all handling is performed in liquid nitrogen or in its vapour. Within 0.1 mm all crystals we used for the structure determination at the different temperatures had approximately the size $0.3 \times 0.4 \times 0.7\,\text{mm}^3$.

For the *data collection at* 80 *K*, 115 *K and* 165 *K* we used a cryostat mounted on a two-arc diffractometer (Siemens) and a conventional X-ray tube. CuK_α-radiation was filtered by a graphite monochromator. The cryostat is built up by a number of concentric stainless steel tubes and a vacuum of about 10^{-5} Torr is used for thermal isolation of the sample. The inner tube contains the gonimeter head mounted on a rod which allows rotation through 360°. A stream of cold nitrogen vapour cools the crystal and regulation of the vapour flow allows working temperatures between 80 K and 300 K to be stabilized with an accuracy of $\pm$ 2 K. The X-ray beam has to pass 4 mylar windows. For CuK_α-radiation these windows limit the resolution to 2.6 A parallel to the rotation axis and to 2.0 A perpendicular to it, the maximum resolution on the diagonal is 1.8 A. Debye rings from the mylar windows were suppressed by carefully adjusting screens. The intensity measurements were carried out photographically using the oscillation method and a cylindrical film cassette with 3 films in a pack. The oscillation angle of each exposure was between 2.5° and 6.0° and the total measurement covered a range of 180°. After data evaluation of the 80 K measurement we found that the oscillation angles chosen were too large in this case, giving avoidable overlap of reflexions. For this reason the number of reflexions at 80 K is smaller than at higher temperatures. One crystal for each temperature was used. There was no evidence of any radiation damage to any of the crystals.

The *intensity measurements at* 185 *K* were performed at the EMBL outstation, Hamburg, using synchrotron radiation from the storage ring DORIS. A wavelength of 0.951 A was selected by a silicon monochromator. The film data were collected with a modified Arndt-Wonacott camera with flat film-cassettes. We used three films per exposure separated by steel foils (NIROSTA) of a thickness of 20 μm to gain enough attenuation at this short wavelength. The crystal was cooled by cold N_2 gas in a device developed by Bartunik and Schubert (1982). Three crystals were used to measure reflexion data over a rotation range of about 110°. The absorption factors were determined to be 1.5 for the KODAK NS2-T-film and 3.85 for the steel foils.

Film evaluation and data analysis

Still photographs were used for refinement of the cell constants (Nyborg and Wonacott 1977) and for the

crystal alignment (Schwager and Bartels 1975). The rotation photographs were evaluated with the program FILME (Schwager and Bartels 1977). Only fully recorded reflexions above the 2.5 significance level were taken into account. The dataset collected with synchrotron radiation was evaluated using 0.92 for the horizontal fraction of polarization. Scaling of the different exposures was done using the program system PROTEIN (Steigemann 1974). Only linear scale factors were applied. Table 1 shows the number of measurements, independent reflexions, N_{indep}, and R_{merge}-values as a measure of the quality of the datasets. The R_{merge}-values are defined as:

$$R_{\text{merge}} = \frac{\sum_{j=1}^{N} \sum_{i=1}^{m_j} |\langle I \rangle_j - I_i|}{\sum_{j=1}^{N} m_j \langle I \rangle_j}, \quad (1)$$

where $\langle I \rangle_j$ is the averaged intensity of the independent reflexion j, where m_j individually measured intensities I_i contribute.

For the *refinement of the structures* we used the restrained refinement procedure in reciprocal space of Hendrickson and Konnert (Konnert 1976; Konnert and Hendrickson 1980) modified so that different occupancies of one or two alternative positions of residues were allowed.

The physical idea behind this method of applying restraints on the individual mean-square displacements, $\langle x^2 \rangle$, is that the $\langle x^2 \rangle$-values of two bonded atoms are not independent of each other but should be rather similar. The advantage is that even at medium resolution meaningful individual mean-square displacements can be refined. The weight of these restraints can be controlled by the input parameter σ_b, the expected variance of $(\langle x_a^2 \rangle - \langle x_b^2 \rangle)$, where a and b are two atoms bound to each other. The actual tightness of the restraints also depends on other quantities such as resolution range and weighting of the reflexions (crystallographic residual). Because of these considerations it is better to use the actual variance, r_B, which is defined as

$$r_B = \sqrt{\frac{1}{N} \sum_{i=1}^{N} (B_a - B_b)_i^2}, \quad (2)$$

with $B = 8\Pi^2 \langle x^2 \rangle$ and where a and b are two atoms of the covalent bond i and N is the number of bonds.

As starting models for the refinement of the low temperature structures we took the coordinates of the already refined 300 K Mb-structure including 160 H_2O molecules and two sulphate ions (Hartmann et al. 1986) and overall temperature factors obtained from Wilson plots.

The general strategy of the refinement was the same for all structures, the number of necessary refinement cycles to reach a certain stage in the refinement differed, however. For the first few cycles, reflexions above a resolution of 2.5 A were excluded to get a greater convergence range for the procedure. Only coordinates and an overall B-value were refined. After typically five cycles the resolution was gradually increased and at a resolution of 2 A individual isotropic mean-square displacements were refined for each of the non-hydrogen atoms. The refinement of each structure was now continued in two parallel ways with different restraints on the individual mean-square displacements. In one type of refinement we tried to make r_B as equal as possible for all structures from 80 K to 300 K (case A in Table 2). In a second attempt we tried to give r_B the same temperature dependence as the overall B-value (case B in Table 2). The truth should be between these extreme assumptions. In both cases we performed the same number of refinement cycles. Table 2 shows the r_B-values, separated for backbone and side-chains, and standard R-values for cases A and B at the end of the refinement, as well as some

Table 1. Parameters of structure determination at the temperature T; N_{obs}, number of the measured reflexions; N_{indep}, number of the independent reflexions; R_{merge} is defined by Eq. (1)

T [K]	80	115	165	185	300
N_{obs}	17,965	31,643	32,464	34,421	56,864
N_{indep}	4,589	9,168	8,261	12,283	15,903
R_{merge}	0.104	0.053	0.055	0.061	0.052
Resolution [Å]	2.0	1.8	1.8	1.5	1.5

Table 2. Parameters for the refinements A and B (see the text). r_B (back) and r_B (side) are defined by Eq. (2). r_D, r_A, r_p, r_w are the rms-deviations of the model from standard distances, dihedral angles, planes and van der Waals distances which are equal for cases A and B. The last line gives the total number of refinement cycles which were equal for the refinements A and B

		80 K	115 K	165 K	185 K	300 K
	r_B (back) [Å]	1.07	1.11	1.16	1.10	1.13
A	r_B (side) [Å]	1.10	1.21	1.24	1.24	1.43
	standard R-value	0.158	0.184	0.185	0.188	0.181
	r_B (back) [Å]	0.78	0.90	1.03	1.07	1.24
B	r_B (side) [Å]	0.82	1.05	1.21	1.32	1.71
	standard R-value	0.163	0.178	0.188	0.189	0.176
Resolution [Å]		5.2–2.0	5.5–1.8	5.5–1.8	5.5–1.5	5.5–1.5
Reflexions		4,503	9,017	8,072	12,118	15,536
r_D [Å]		0.015	0.018	0.017	0.017	0.015
r_A [Å]		0.081	0.076	0.079	0.064	0.068
r_p [Å]		0.011	0.013	0.011	0.013	0.014
r_w [Å]		0.17	0.16	0.16	0.17	0.15
Cycles		28	28	28	24	16

Table 3. Cell constants of Mb_{met} at different temperatures

T [K]	a [Å]	b [Å]	c [Å]	β [°]
300	64.52 ± 0.03	30.90 ± 0.01	34.85 ± 0.02	105.80 ± 0.02
185	64.04 ± 0.07	30.73 ± 0.04	34.29 ± 0.05	105.70 ± 0.06
165	63.81 ± 0.06	30.73 ± 0.02	34.26 ± 0.04	105.65 ± 0.04
115	63.80 ± 0.03	30.68 ± 0.01	34.26 ± 0.02	105.66 ± 0.02
80	63.60 ± 0.11	30.52 ± 0.05	34.11 ± 0.08	105.60 ± 0.05

refinement parameters common to both cases. After about ten refinement cycles with individual mean-square displacements there was no further improvement of the R-value. At this stage ($2F^o - F^c$)-maps were calculated and inspected on a vector display using the program FRODO (Jones and Liljas 1984). Misplaced atoms could not be detected. At 185 K and 165 K we found alternate conformations for LEU 61 and LYS 63, already detected for the structure at 300 K (Hartmann et al. 1986). The new positions were built into the models of the 165 K- and 185 K-structures and an additional six cycles of refinement were performed, allowing variable occupancies for the disordered atoms of LEU 61 and LYS 63. Finally ($F^o - F^c$)-maps were calculated for all structures. The total number of refinement cycles is given in Table 2.

Using equal weights, r_B, for backbone and side-chains, constant r_B-values for all temperatures could only be reached for the backbone (case A in Table 2). While at low temperatures r_B is approximately the same for backbone and side-chains, at 300 K r_B is considerably greater for the side-chains.

Upon reducing the temperature the unit cell of myoglobin shrinks. Cell constants at various temperatures are given in Table 3. On average the reduction between 300 K and 80 K is less then 2%. Before a refinement of the structures at different temperatures this shrinking was taken into account.

In a number of proteins it was found that side-chains can occupy two or more positions which can be clearly distinguished in the density map. An inspection of myoglobin showed two pronounced examples of different positions of side-chains, namely LEU 61 and LYS 63. While at low temperatures only one position is occupied, at higher temperatures two or three positions are populated.

The number of side-chains with clearly different positions is astonishing small. No indications for other well defined different positions were found although the N terminus is not well ordered until GLN 8 (Takano 1977a). A more careful analysis could increase the number of residues which occupy different positions. Nevertheless, the present results show that an analysis of the structural distributions assuming a Gaussian around the average position is a reasonably good approach.

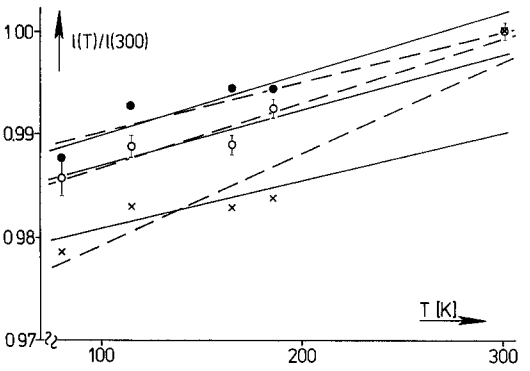

Fig. 1. Thermal expansion of the crystal lattice as a function of temperature. The lattice parameters $l(T) = a, b, c$, respectively, are normalized to 300 K. *Open circles:* a/64.52; *closed circles:* b/30.90; *crosses:* c/34.85. *Solid lines* and *dashed lines* give the linear regression taking into account only measurements below 200 K and at all temperatures, respectively

Results and discussion

The temperature dependence of lattice parameters

Upon lowering the temperature the lattice parameters **a**, **b**, and **c** of the myoglobin crystal are reduced. Figure 1 gives the relative changes of the cell dimensions normalized to $T = 300$K. The dashed lines give the linear regression to all temperature data. While it describes the temperature dependence of **a** and **b** reasonably well, **c** clearly does not vary linearly with temperature. The solid lines include only data from 80 K to 185 K in the linear regression. In this region the **c**-axis also shows a change proportional to the temperature. The experimental value at 300 K, however, differs markedly from the extrapolation of this fit to 300 K. Within the limitations of the present experiments the behaviour of the **c**-axis indicates some type of phase transition above 185 K. It should be mentioned that trials to determine the myoglobin structure at about 200 K failed because the crystal cracked after some hours. A change of dynamic parameters was also found from Mössbauer experiments (compare Parak et al. 1982) in this temperature region.

The temperature dependence of the average structure

Having corrected the atomic coordinates of the molecule for the thermal expansion of the crystal lattice one can then look at the temperature dependence of the average structure. The thermal expansion of myoglobin has already been discussed elsewhere (Frauenfelder et al. 1987). This work was, however, based only on structures at 80 K and 300 K and here we would like to discuss some additional features.

To get an idea of the structural changes one can project the atomic coordinates on a plane and compare the results for different temperatures. It can easily be seen that the gross structure remains essentially the same although small changes of coordinates do occur. A quantitative comparison has been performed in the following way. First the 115 K structure was normalized to the unit cell dimensions of the 300 K structure and than rotated so that the backbone atoms coincided as well as possible. Then, average coordinates $\bar{R}(T)$ of the N–C–C backbone atoms of each residue were calculated for both structures. The squared changes of coordinates, $\Delta\bar{R}^2$ were calculated according to:

$$\Delta\bar{R}^2 = (\bar{R}_a - \bar{R}_b)^2 \tag{3}$$

where the subscripts a and b refer to $T = 300$ K and $T = 115$ K, respectively.

In Fig. 2 $\Delta\bar{R}^2$ of the backbone atoms is shown as a function of the residue number (full circles). For comparison, the mean square displacements, $\langle x^2 \rangle$, of met-Mb are shown in the same figure (open circles taken from Hartmann et al. 1986). The $\Delta\bar{R}^2$-values show a correlation with the $\langle x^2 \rangle$-values. Large changes occur where the distribution of coordinates is large. For the average over all residues, $\Delta\bar{R}^2$ is smaller than $\langle x^2 \rangle$ ($\Delta\bar{R}^2 = 0.036$ A^2; $\langle x^2 \rangle = 0.144$ A^2). At all positions the change of the coordinates induced by cooling occurs within the distribution of coordinates at 300 K. The average structure at 115 K already exists at 300 K but with a lower weight.

To get a better impression of the structural change induced by cooling we compare it with the conformational change between Mb_{met} and Mb_{deoxy}. The procedure to get the coordinates is as described. Again, Eq. (3) is used but now the subscripts a and b refer to the coordinates of Mb_{met} and Mb_{deoxy}, respectively, where the Mb_{deoxy} data were taken from Phillips (1980). Crosses in Fig. 2 give the $\Delta\bar{R}^2$-values characterizing the conformational change from Mb_{met} to Mb_{deoxy}. At nearly all positions it is smaller than the structural distributions of Mb_{met} at room temperature. Exceptions occur close to the FG-loop (residues 98-103) and at position 120 in the GH-loop. Within structural distributions of the backbone the room temperature structure of Mb_{met} contains the Mb_{deoxy} structure but with lower weight. Conformational changes of the molecules shift the average coordinates within the distribution of coordinates of one specific conformation.

A similar comparison of side-chain average coordinates again yields a correlation of distributions within the 300 K structure and structural changes by freezing or a change from the met to the deoxy conformation. While the mean square structural changes between Mb_{met} at 300 K and 115 K exceed the structural distributions in only a few cases, the $\Delta\bar{R}^2$-values between

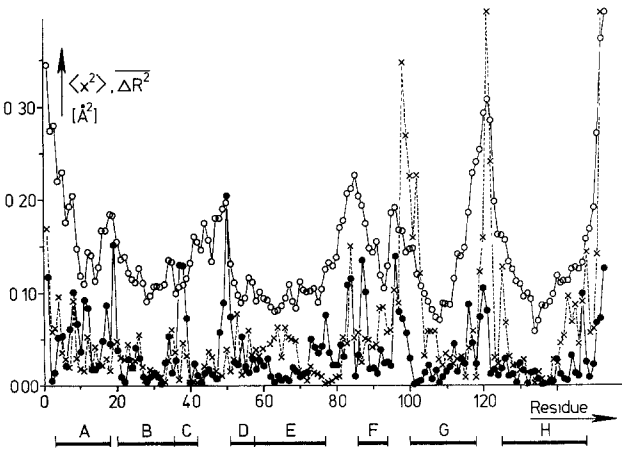

Fig. 2. *Closed circles:* Mean-square changes, $\Delta\bar{R}^2$, of the average coordinates of the backbone atoms by cooling from 300 K to 115 K as a function of the residue number. The *open circles* are for comparison and give the mean-square displacements of the backbone atoms at 300 K taken from Hartmann et al. (1986). *Crosses* give $\Delta\bar{R}^2$-values between the metmyoglobin and the deoxymyoglobin structure at 300 K

the Mb_{met} and Mb_{deoxy} structure are very large. Conformational changes are mainly reflected by shifts of the side-chains.

Comparing the transition met–deoxy and 300 K – 115 K a correlation of the $\Delta\bar{R}^2$-values could be assumed, especially in the E to H part of the molecule. A comparison of the $\Delta\bar{R}^2$-values of Mb_{met} at 115 K and Mb_{deoxy} shows, however, that freezing does not shift the Mb_{met} structure in the direction of the Mb_{deoxy} structure. With respect to the backbone the 115 K Mb_{met} structure and the Mb_{deoxy} structure is within the distribution of the 300 K Mb_{met} structure but at different average coordinates.

Different positions of side-chains and oxygen access to the heme pocket

Well resolved alternative positions of side-chains were found only for LEU 61 and LYS 63. Figure 3 shows the electron density around LEU 61 for the 300 K structure. The density values are calculated by a $(2F^o - F^c)$-synthesis. All the atoms labeled in Fig. 3 have been included in the calculation of the F^c-values. There is clearly a third peak (C in Fig. 3) for the two side-chain atoms CD1 and CD2. This is consistent with alternative positions of the side-chain, separated by rotations of about 120° and 240° around the CB–CG bond (torsion angle χ_2). The main conformation already known from the literature (Takano 1977a; Frauenfelder et al. 1979), is drawn with solid lines in Fig. 3 and labeled with 1.

$(2F^o - F^c)$-maps of the low temperature structures gave a reduced electron density for peak C at

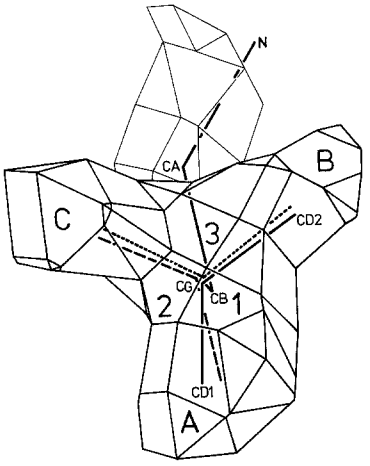

Fig. 3. Electron density cage around the side-chain of LEU 61, calculated by a $(2F^o - F^c)$-synthesis. The density level is 0.5 e/A^3. The letters *A* to *C* mark the three density peaks produced by the alternate conformations 1, 2 and 3 of the side-chain. The different conformations are produced by rotations of about 120° around the CB–CG bond. Conformations 1, 2 and 3 are drawn with *full*, *dashed* and *dotted lines*, respectively

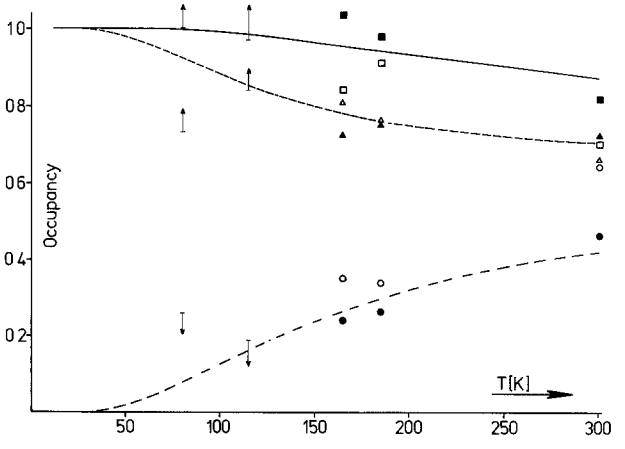

Fig. 4. Occupancies of different side-chain positions of LEU 61 as a function of temperature. Positions *A*, *B* and *C* (compare Fig. 3) are marked by *squares*, *triangles* and *circles*, respectively. Open symbols refer to occupancies estimated from peak electron densities while full symbols give the result of refinements. For 80 K and 115 K only lower and upper limits can be given. Assuming a three state model where the states differ in energy, the occupancies can be calculated. With energies of 1.7 and 3.8 kJ/mol for conformation 2 and 3 the *solid*, *dashed* and *dash-dotted lines* give calculated occupancies for position *A*, *B* and *C*, respectively

185 K and 165 K and no significant density for this position at 115 K and 80 K, indicating that the alternative positions of LEU 61 can be frozen out. To get a better estimation of the occupancies of the three positions, $(F^o - F^c)$-maps were calculated at all temperatures. Atoms CD1 and CD2 were excluded from the models to allow a direct comparison of the densities at positions *A*, *B* and *C*.

To a first approximation, peak electron densities can be taken as a measure of relative occupancies. The sum of the occupancies of the three positions should be equal to 2.0, because there are no indications for further conformations of LEU 61 even at the noise level of the difference maps which is less than about 0.1 e/A^3 for all temperatures. Normalizing the sum of the relative occupancies to 2.0, absolute values of the occupancies can be calculated. The results are shown in Fig. 4 (open symbols). Since for 115 K and 80 K no density could be found at position *C* only upper limits have been given together with the corresponding lower limits for positions *A* and *B*.

For 300 K, 185 K and 165 K data a refinement was performed allowing different occupancies for positions *A* to *C*. Results of these refinements are shown as closed symbols in Fig. 4. Discrepancies to the estimations from the peak density come from the fact that the conformers 1, 2 and 3 do not give identical positions *A*, *B* and *C*. Especially for position *A* the peak density underestimates the occupancy because the position of CD1 is separated by 0.4 A in comparing conformation 1 and 2.

In order to estimate relative energies between the three side-chain positions of LEU 61 a simple model was used where conformation 2 and 3 have an energy of ε_2 and ε_3 with respect to conformation 1. Calculations using $\varepsilon_2 = 1.7$ kJ/mol and $\varepsilon_3 = 3.8$ kJ/mol give a good agreement with the measured occupancies of the different positions (compare lines in Fig. 4). While ε_2 is quite well defined by the experiment ($\pm$ 0.05 kJ/mol) test calculations show that ε_3 can vary between 2.67 and 5.55 kJ/mol and still explain the experimental data.

It is well known that the conformation of myoglobin obtained as the average structure of about 10^{15} molecules does not allow an unhindered entrance of the oxygen molecule into the heme pocket. Case and Karplus (1979) have investigated different paths. A direct path from the solvent to the heme pocket is restricted mainly by the distal histidine. Ringe et al. (1984) have shown that phenylhydrazine binds to the iron in a way that HIS 64 (E7), ARG 45 (CD3) and VAL 68 (E11) are forced aside to form an open channel to the surface. This suggests that the oxygen could also open this channel. A secondary path for the oxygen is between the *B* and the *E* helix. The only significant energy barrier is caused by the bottle-neck between LEU 61 (E4) and PHE 33 (B14). In their Fig. 11 Case and Karplus (1979) give a diagram discussing the energy of the side-chain of LEU 61 (E4) if rotated around the bond CA–CB (angle χ_1) and around the bond CB–CG (angle χ_2). Our conformations 1 and 2 (compare Fig. 3) come close to the contour line of 0 kJ/mol

(conformation 1: $\chi_1 = 183°$, $\chi_2 = 162°$; conformation 2: $\chi_1 = 179°$, $\chi_2 = 61°$). The value ε_2 is in quite reasonable agreement with this picture taking into account the errors of calculations and experiments. Conformation 3 ($\chi_1 = 185°$, $\chi_2 = 286°$) is in a region of higher energy which is between 8 and 40 kJ/mol, a value which is higher than our experimentally determined value of ε_3. It is interesting to note that the conformation found by Takano (1979a) with $\chi_1 = 165°$ and $\chi_2 = 157°$ is not identical with our conformation 1 but has an energy of about 6 kJ/mol in the diagram of Case and Karplus. Our refinement with alternative positions of LEU 61 side-chains give a better agreement with theory. In this context it should be noted that the coordinates for LEU 61 in Mb_{deoxy} given by Takano (1977b) agree with conformation 1, whereas Phillips (1980) found a conformation for LEU 61 in Mb_{deoxy} similar to conformation 2.

In conformation 1 the bottle-neck for the oxygen passage is formed by the CD1 atom of LEU 61 and the CE2 atom of PHE 33 with a centre to centre distance of 4.26 A. In conformation 2 this distance is not changed while in conformation 3 the distance increases to 4.78 A, and the CG atom of LEU 61 determines the smallest passage. The next limitation of the entrance channel is formed by LEU 61 CD2 and PHE 33 CE2 if the molecule is in conformation 3. Upon jumping back to conformation 1 this hindrance disappears. Therefore, the most favourable condition for the passage occurs if the side-chain of LEU 61 jumps between conformation 1 and 3 during the O_2 passage, in this way reducing the energy barrier which the O_2 molecule has to overcome. Nevertheless, steric hindrance still occurs because the Van der Waals radius of C-atoms is at least 1.6 A and the radius of the O_2 molecule at least 1.4 A. However, one has to have in mind that the $\langle x^2 \rangle$-values of the side-chains of LEU 61 and PHE 33 are 0.125 A^2 and 0.100 A^2, respectively. This means that in a number of molecules the channel is much wider and the barrier for the oxygen is further reduced.

The Gaussian approximation for mean square displacements

X-rays structure analysis yields mean coordinates of the atoms of a molecule as an average over all unit cells of the crystal. Displacements **u** from these coordinates, not resolved as well defined different positions, may stem from static or dynamic effects. In the data analysis it is assumed that the distribution of coordinates around the mean coordinates is Gaussian and isotropic. A normalized Gaussian distribution is defined as

$$G^G(\mathbf{u}, t) = (2\,\Pi\, w(t))^{-3/2} \exp\left[-u^2/(2\,w(t))\right]. \quad (4)$$

The mean-square displacement, $\langle u^2 \rangle$, becomes then

$$\langle u^2 \rangle = \int_{-\infty}^{+\infty} u^2\, G^G(\mathbf{u}, t)\, dx\, dy\, dz = 3w(t). \quad (5)$$

With independent displacements in the directions of the Cartesian coordinates one gets

$$3\,w(t) = \langle x^2 \rangle + \langle y^2 \rangle + \langle z^2 \rangle. \quad (6)$$

The assumption of isotropic displacements with $\langle x^2 \rangle = \langle y^2 \rangle = \langle z^2 \rangle$ yields

$$w(t) = \langle x^2 \rangle. \quad (7)$$

Note, that the Gaussian approximation is not correlated with the magnitude of $\langle x^2 \rangle$. Assuming a Gaussian density distribution in space is not concerned with the time dependence of motions.

Linear regression of the temperature dependence of $\langle x^2 \rangle$

Frauenfelder et al. (1979) found that the temperature dependence of the $\langle x^2 \rangle$-values of Mb averaged over the backbone or side-chain atoms of a residue indicate rather anharmonic potentials which govern the dynamics of myoglobin. These discussions were, however, based on a rather limited temperature interval between 225 K and 300 K. Investigations at 80 K (Hartmann et al. 1982) have modified the picture and have indicated that for a large number of residues $\langle x^2 \rangle$ decreases linearly with temperature. In order to get a clear picture an error analysis has been performed comparing $\langle x^2 \rangle$-values of Mb_{met} determined from different experiments (Hartmann et al. 1986) yielding error bars of $\pm\,\sigma = 0.01 + 0.1\langle x^2 \rangle$ for the $\langle x^2 \rangle$-values. In the following $\langle x^2 \rangle$ was tentatively assumed to be proportional to T. The results of the different refinements (case A and B) for the 153 residues are treated separately and the results of case A are given in brackets. A linear regression showed that all experimental data were within $\pm\,\sigma$ for 131 (139) backbone averages and 102 (110) side-chain averages while for 17 (6) backbone averages and 28 (23) side-chain averages the $\langle x^2 \rangle$-values at 4 temperatures were within $\pm\,\sigma$ and at one temperature within $\pm\,2\sigma$. It is obvious that the number of residues showing a distribution linearly decreasing with temperature do not significantly depend on the refinement procedure.

Figures 5 to 7 give examples from the temperature dependence of $\langle x^2 \rangle$-values which will be discussed later.

Approximating the temperature dependence of the $\langle x^2 \rangle$-values of backbone and side-chains by straight lines allows a linear extrapolation to $T = 0$ K and an interpolation yielding values at $T = 300$K. At first sight a linear extrapolation to $T = 0$ seems rather un-

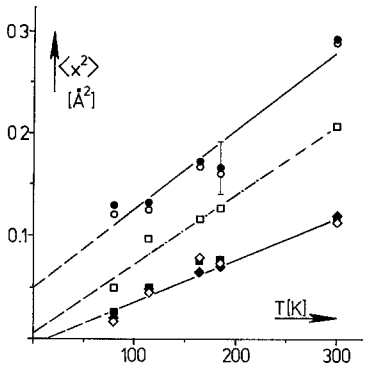

Fig. 5. Mean-square displacements averaged over the backbone atoms NCC (*full symbols*) and side-chains atoms (*open symbols*) as a function of temperature. *Solid lines* and *dash-dotted point lines:* linear regression of backbone and side-chain values, respectively; *dashed lines:* extrapolation to $T = 0$ K; *circles:* PRO 120 (GH 2); *squares:* LYS 56 (D6); *diamonds:* THR 39 (C4)

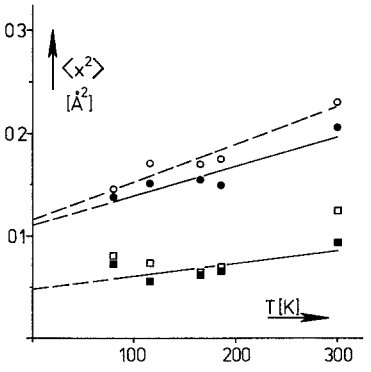

Fig. 6. As in Fig. 5. *Circles:* LEU 86 (F1); *squares:* LEU 61 (E4)

physical. At low temperature zero point vibrations exist and the slope of any function describing the temperature dependence of the $\langle x^2 \rangle$-values has to disappear. Nevertheless, the linear extrapolation yields a lower limit for the $\langle x^2 \rangle$-values at 0 K. Figure 8 a and b show the result of this extrapolation for the backbone and the side-chains, respectively. We shall come back to a discussion of these figures later. Here we note only that almost no $\langle x^2 \rangle$-average values at $T = 0$ K are below zero. The few exceptions can be understood from the error bars and from the fact that these values are only lower limits of the true values.

Rotational and translational displacements of the entire molecule

Before discussing intramolecular dynamics one has to ask if the mean-square displacements can be understood in a simple model of intermolecular motions. In the simplest picture one can assume rotations and

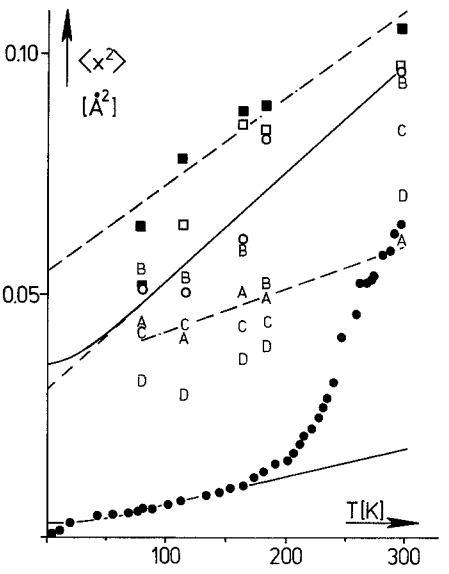

Fig. 7. Mean-square displacements as a function of temperature. *Circles:* Fe; *full symbols:* $\langle x^2 \rangle^{\gamma}_{Fe}$ measured by Mössbauer spectroscopy, *solid line:* Debye law for ^{57}Fe with $\theta^{\gamma} = 195$ K; *open symbols:* $\langle x^2 \rangle^{x}_{Fe}$ determined by X-ray structure analysis; *solid line:* Debye law for Fe with $\theta^{x} = 107$ K shifted to fit the slope of the experimental data. *Closed* and *open squares:* $\langle x^2 \rangle$-values of the backbone and the side-chain averages of the proximal HIS 93, respectively. *A*, *B*, *C*, *D*: $\langle x^2 \rangle$-values averaged over the atoms of the four pyrrolls 3, 4, 1, and 2, respectively. *Dash-dotted lines:* linear regression to *A* and full squares, respectively. *Dashed lines:* linear extrapolations

translations of the entire molecule with respect to its centre of gravity.

A pure rotational motion modifies Eq. (6). If Z is the distance from the centre of gravity and the displacements are perpendicular and proportional to Z one obtains

$$3\,w(t) = C\,Z^2 = 2\langle x^2 \rangle_Z\,. \tag{8}$$

Here, $\langle z^2 \rangle$ of Eq. (6) equals zero.

Figure 9 gives $\langle x^2 \rangle$-values averaged over shells between Z and $Z + \Delta Z$ containing about 40 atoms as a function of the distance Z from the centre of gravity. A least squares fit of

$$\overline{\langle x^2 \rangle_Z} = A + B\,Z^2\,. \tag{9}$$

yields a good description of the experimental results (solid lines in Fig. 9). It should, however, be mentioned that a linear increase of $\langle x^2 \rangle$ with Z being physically meaningless also gives a good fit.

Figure 10 analyzes the consequences of the assumption of a rigid sphere libration. The squares once more give uncorrected $\langle x^2 \rangle$-values of the backbone averages at 300 K. Depending on their distances Z from the centre of gravity of the molecules these values were diminished by $\overline{\langle x^2 \rangle_Z} - A$. Closed and open circles in Fig. 10 give the results of this correction for 300 K

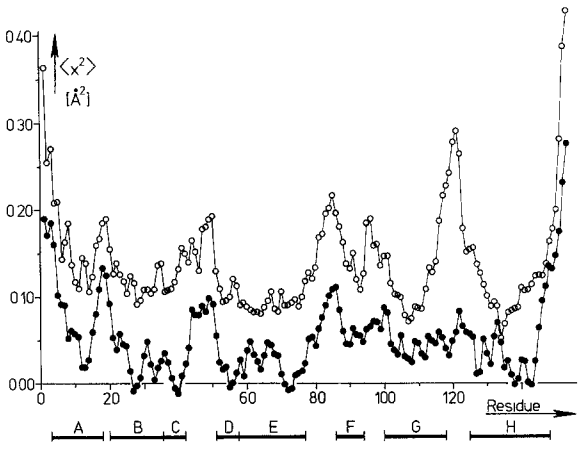

a

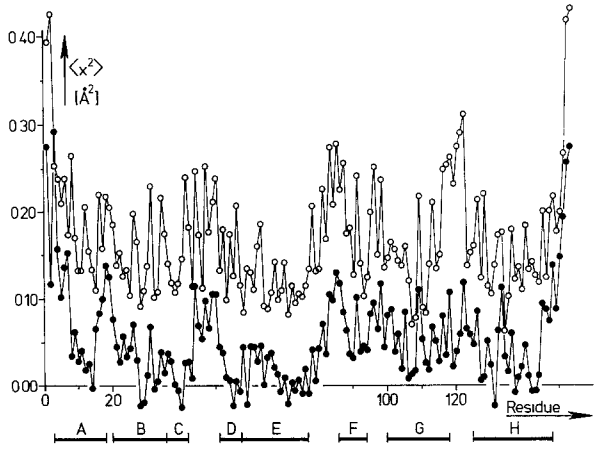

b

Fig. 8a and b. Mean-square displacements of the backbone atoms (**a**) and side-chain atoms (**b**) from a linear regression of the measurements at 5 different temperatures. *Open circles:* interpolation to 300 K. *Full circles:* linear extrapolation to 0 K

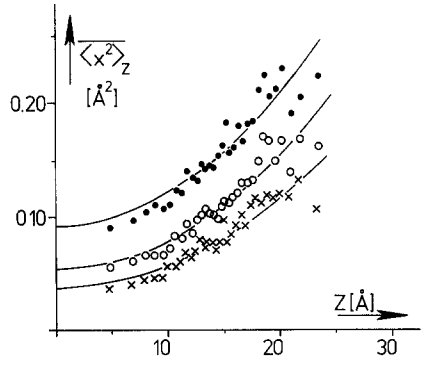

Fig. 9. Values of $\langle x^2 \rangle$ averaged in shells with distance Z from the centre of gravity of the molecule. Each shell contains about 40 atoms. *Full circles:* $T = 300$ K; *open circles:* $T = 185$ K; *crosses:* $T = 80$ K. The *solid lines* give a least squares fit of Eq. (8) assuming a Z^2-dependence

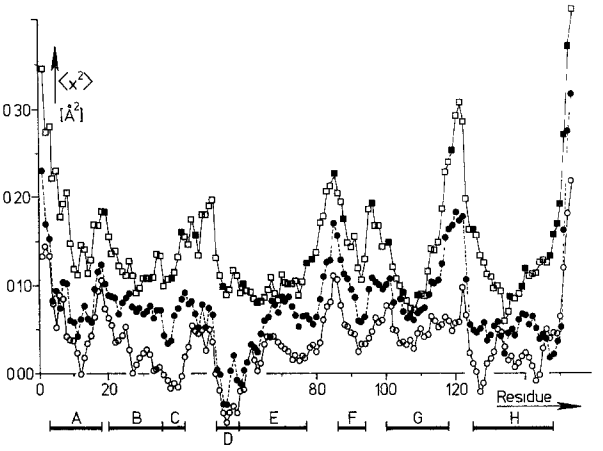

Fig. 10. Mean-square displacements averaged over backbone atoms as a function of the positions in the sequence. *Squares:* $T = 300$ K, without any correction; *full squares:* contacts to neighbouring molecules; *circles:* rigid spheres correction rotational modes only; *closed circles:* $T = 300$ K; *open circles:* $T = 80$ K. For details see the text

and 80 K data, respectively. Comparing the 300 K values it is obvious that the corrections change the general picture mainly in the region of the *D*-helix. In all other parts of the molecule the principal picture remains the same: large disorder in loops, smaller disorder in the helices. Only the absolute values are diminished. The negative $\langle x^2 \rangle$-values of the *D*-helix show that at least in this region an overcorrection has been performed. It is obvious that the correction becomes worse in regions where one molecule is bound to a neighbour because librations are hindered. Intermolecular contacts are indicated by full squares. Such contacts occur in many parts of the molecule and are not specific for the *D*-helix. Therefore, they cannot be used as an explanation for the negative $\langle x^2 \rangle$-values in the *D*-helix.

Correcting the $\langle x^2 \rangle$-values by a rigid molecule translational motion means a subtraction of the parameter A obtained from Eq. (9). In this case many $\langle x^2 \rangle$-values at 300 K and even more at 80 K become negative. These negative values are clearly outside the error bars.

Squares and circles in Fig. 10 represent two extreme cases: In the first picture no disorder stems from displacements of the molecule as the whole. In the alternative picture we tried to understand disorder by displacements of the entire molecule. Both pictures describe only parts of the physical reality. The relative weight of the two extreme cases cannot be determined at present. In the following discussions rotational and translational movements of the entire molecule are neglected. The arguments in favour of this procedure are summarized in the following: *(i)* The correction with rotational and translational disorder produces

too many negative $\langle x^2 \rangle$-values at 80 K. This means that these contributions are drastically overestimated. *(ii)* If librations dominate, at least some influence of intermolecular contacts should be seen. *(iii)* A possible correction with the right weight does not change the arguments in the following discussions. Only the absolute values are modified. All corrections are linear with temperature. *(iv)* There are results from Mössbauer investigations on model compounds which also favour the picture of intramolecular dynamics (Parak et al. 1987b). It is, however, important to keep in mind that rotational and translational motion may exist to some extent when comparing absolute $\langle x^2 \rangle$-values with theoretical investigations such as molecular dynamics calculations (Levy et al. 1985).

Comparison with results from Mössbauer spectroscopy

The mean-square displacements of the iron in myoglobin, $\langle x^2 \rangle_{Fe}$, can be determined by X-ray structure analysis ($\langle x^2 \rangle^x_{Fe}$) and Mössbauer absorption spectroscopy ($\langle x^2 \rangle^\gamma_{Fe}$). Due to the different time sensitivity of the two methods the $\langle x^2 \rangle_{Fe}$-values differ as shown in Fig. 7. Within the limits of experimental errors the temperature dependence of $\langle x^2 \rangle^x_{Fe}$ is linear while strong deviations from a linear temperature dependence occur for the $\langle x^2 \rangle^\gamma_{Fe}$-values above 200 K. A linear temperature dependence of mean-square displacements in a larger temperature interval suggests a Debye behaviour according to

$$\langle x^2 \rangle = \frac{3}{4} \frac{\hbar^2}{k_B/3} \frac{1}{m} \frac{1}{\Theta} \left[1 + 4 \left(\frac{T}{\Theta} \right)^2 \int_0^{\Theta/T} \frac{Z \, dZ}{e^Z - 1} \right]. \qquad (10)$$

Here $\hbar$ is the Planck constant divided by 2Π, k_B the Boltzmann constant, m the mass of the vibrating atom and θ the Debye temperature. It is well known that the Debye model is an oversimplification for most of the cases where it is applied. Nevertheless, it is a generally accepted method to describe vibrations of solids by only two parameters. The solid lines give fits of Eq. (10) to $\langle x^2 \rangle^x$ and $\langle x^2 \rangle^\gamma$, respectively. In both cases only the slopes of the experimental data were taken into account. The fit of the $\langle x^2 \rangle^x$-values is valid only after subtraction of 0.03 A^2 from the experimental data. For $\langle x^2 \rangle^\gamma$ all values above 180 K have been neglected. X-ray measurements yield a Debye temperature $\theta^x = 107$ K; from Mössbauer data one obtains $\theta^\gamma = 195$ K. The present results can be compared with results obtained from measurements of the second order Doppler shift of iron in myoglobin (Reinisch et al. 1985). Excellent agreement with the Debye temperature θ^γ is obtained. As shown by Reinish et al. (1985) the second order Doppler shift can be understood assuming $\theta \approx 200$ K in the temperature range between 4.2 K and 300 K. No peculiarities occur above $T = 200$ K. A Debye temperature of 195 K is representative of the binding of the iron to its neighbours. It does not reflect slow segmental motions of larger parts of the molecule giving rise to the increase of $\langle x^2 \rangle^\gamma$ above 200 K. While the θ^γ-value obtained from Mössbauer spectroscopy seems to be physically meaningful, the lower θ^x-temperature obtained from X-ray structure analysis cannot be discussed in a consistent way. The fact that Mössbauer spectroscopy neglects frequencies lower 10^{+7} s^{-1} does not explain the differences in the Debye temperatures. The fact that the effective mass for low frequency modes is certainly much larger than the mass of the iron also gives no quantitative explanation. The discrepancy between the Mössbauer and X-ray results is a strong hint that the linear temperature dependence of the $\langle x^2 \rangle^x$-values is not due to a motion in a harmonic potential. A consistent picture is obtained if one assumes that the $\langle x^2 \rangle^x$-values are only sensitive to the envelope of the true potential while the $\langle x^2 \rangle^\gamma$-values measure real motions on a time scale faster 10^{-7} s. Within this envelope the potential has traps with different barriers. The Boltzmann factor gives the relative number of molecules trapped in a conformation where the iron is displaced by $(\langle x^2 \rangle^x)^{1/2}$ from the average position. The linear temperature dependence shows that the whole system is in thermodynamic equilibrium. Below 200 K the iron is limited to one trap for more than 10^{-7} s. Vibration occurs only within this conformation. Above 200 K the molecule is flexible enough to change the conformation on a time-scale faster than 10^{-7} s. In this way the iron explores larger parts of the whole potential which is measured by Mössbauer spectroscopy.

A potential way of explaining X-ray and Mössbauer results in a consistent way was given by Parak and Knapp (1984). The present analysis proves the accuracy of the experimental basis of this picture. Nevertheless, other potentials may also give a consistent interpretation of the data. The discussions are still in a preliminary state (compare for instance Frauenfelder 1985 and Parak et al. 1987b).

A generalization of the results obtained at the iron is reasonable since the iron shows no peculiarities with respect to the residues in Mb. Moreover, it is proved that it moves together with its neighbours (Parak et al. 1982), labeling protein dynamics of segments of the molecule. A generalization is also supported by RSMR-experiments (Krupyanskii et al. 1982; Nienhaus and Parak 1986).

Discussion of structural distributions within myoglobin; the low temperature limit

The examples shown in Figs. 5 and 6 are representative of the temperature dependence of structural disor-

der. PRO 120 is situated in the GH corner and belongs to the residues with the largest $\langle x^2 \rangle$-values. In the figure average values of the backbone N–C–C-atoms and of the side-chain atoms are shown separately. The mean square displacements of the backbone atoms and the side-chain atoms are very similar. This is also the case for the other prolines in myoglobin, reflecting the fact that in this residue the side-chain is bound two times to the backbone.

Side-chain averages can show more or less disorder than backbone averages. In many cases the temperature dependence is such that the extrapolation to 0 K gives very similar values for backbone averages and side-chain averages of one residue (compare LYS 56 and LEU 61 in Figs. 5 and 6 respectively). This holds also for the averages over all backbone atoms and all side-chain atoms in myoglobin as shown in Fig. 11. At higher temperatures side-chains are slightly more disordered on the average.

Comparing the surrounding of the iron (see Fig. 7) the disorder increases on going from the iron to the side-chain of the proximal histidine and to the backbone. Within the heme group the disorder varies (compare pyrrolls *A* to *D*).

More than one third of the water molecules in myoglobin crystals are crystallographically visible at all temperatures. On the average, the disorder is rather high. Lowering the temperature decreases the averaged mean square displacements dramatically (compare Fig. 11).

The temperature dependence of the mean-square displacements proves that the disorder can be partly frozen out. Therefore, it is connected with dynamic processes. A linear temperature dependence is also a clear hint that the system has been in thermal equilibrium during the measurement.

For a molecule with a well defined minimum in energy all atoms should have well defined positions at very low temperatures uncertain only by zero point vibrations. As examples we refer to urea and bis(bipyridyl)dichloroiron-tetrachloroferrate where neutron structure analysis was performed at low temperatures. In urea the mean square displacements averaged isotropically over the C,N- and O-atoms are 0.0165 A^2 at 123 K and 0.0073 A^2 at 12 K (Swaminathan et al. 1984). The iron complex yields $\langle x^2 \rangle$-values of the two irons of 0.0129 A^2 and 0.0212 A^2 at 115 K and 0.0042 A^2 and 0.0060 A^2 at 4.2 K, respectively. The average mean-square displacement of the C and N atoms is 0.0223 A^2 at 115 K and 0.0068 A^2 at 4.2 K. The largest $\langle x^2 \rangle$-value of a C atom is 0.0083 at 4.2 K (Figgis et al. 1983).

As shown in Fig. 8 a linear extrapolation of the $\langle x^2 \rangle$-values of myoglobin to 0 K gives much larger values. Only a few backbone and side-chain averages are close to the values obtained for smaller molecules.

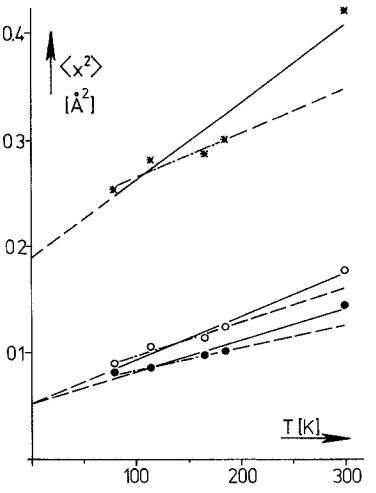

Fig. 11. Averaged mean-square displacements. *Closed circles:* all backbone NCCO-atoms; *open circles:* all side-chain atoms; *stars:* 160 water molecules found crystallographically. *Solid lines:* linear regression; *dash-dotted lines:* linear regression neglecting the values at 300 K; *dashed lines:* extrapolations

The extrapolation to 0 K obviously shows that structural distributions remain present even at very low temperatures. This statement also remains true if one performs a correction for rotational and translational motion. It follows that the energy minimum of the myoglobin structure is not very pronounced.

This behaviour calls to mind low temperature investigations on ice crystals where disorder in the arrangement of protons give rise to a zero point entropy. In proteins, photodissosiation experiments of CO-liganded myoglobin proved the existence of an activation energy spectrum which can be understood by structural distributions (Austin et al. 1975). In an ensemble each individual molecule has a slightly different structure having its individual activation barrier for the rebinding of the CO. It is now common to call these structures conformational substates of a molecule. In this terminology the conformation of a molecule is the mean structure determined by X-ray methods as the average of about 10^{15} molecules while a conformational substate characterizes the structure of an individual molecule of the ensemble. One could also say that conformations of a molecule are different structures which can be resolved by X-ray structure analysis while unresolvable structural differences of molecules determine the conformational distribution.

The present X-ray results are a very direct proof of the concept of conformational substates or conformational distributions.

Within the present accuracy of experimental results there is no justification for discussing a nonlinearity of the temperature dependence of the structural disorder in myoglobin. Nevertheless, there is some hint that the slope of the temperature depen-

dence changes slightly above 200 K. In Fig. 11 mean-square displacements averaged over all backbone atoms, all side-chain atoms and all water molecules, respectively are shown. A linear regression taking into account only values between 80 K and 185 K fits the data better than a linear regression which includes values at 300 K (compare dash-dotted and solid lines). This result is similar to the temperature dependence of the **c**-axis of the myoglobin crystal as shown in Fig. 1 and suggests again some type of phase transition around 200 K. One has, however, to emphasize that averaging over many atoms reduces the error bars only if they behave in the same way, otherwise the error may increase.

As just stated, a small non-linear change of the temperature dependence of the $\langle x^2 \rangle$-values above 200 K is still compatible with the present accuracy of X-ray data. To answer the question of whether such a change in the slope really occurs may be of fundamental importance. Ansari et al. (1985) developed a model which describes the relaxation of the liganded myoglobin to the unliganded. Structural changes go via a well defined number of intermediate states arranged in a hierarchy. Substates belonging to a tier CS^1 are separated by larger potential barries than substates belonging to a tier CS^2 modifying the valleys of tier CS^1 states. The valleys of tier CS^2 are modified by substates of tier CS^3 which in turn are modified by substates of tier CS^4. Experimental evidence is given that equilibrium motions within CS^1 are only possible above 200 K. Although a linear temperature dependence of $\langle x^2 \rangle$-values does not contradict this model even a slight change of the slope of $\langle x^2 \rangle$ versus T above 200 K would strongly support it. Moreover, it would allow us to study many details. Additional structure investigations between 185 K and 300 K are, therefore, necessary. Hopefully, the accuracy of the X-ray data can also be increased in the near future by the use of an area sensitive multiwire proportional counter (Nienhaus et al. 1987).

Comparing our work on a myoglobin crystal with the extended studies of the dynamics of rather simple systems in solid state physics it is obvious that we are at the very beginning of understanding and still deal with rather crude approximations.

This work was supported by the Bundesministerium für Forschung und Technologie, the Deutschen Forschungsgemeinschaft and the Fond der Chemie. One of us (H. H.) wants to thank the EMBO for the grant of a shortterm fellowship. We would like to thank H. Frauenfelder for valuable discussions.

References

Ansari A, Berendzen J, Bowne SF, Frauenfelder H, Iben IET, Sauke TB, Shyamsunder E, Young RD (1985) Protein states and protein quakes. Proc Natl Acad Sci USA 82:5000–5004

Artymiuk PJ, Blake CCF, Grace DEP, Oatley SJ, Phillips DC, Sternberg MJE (1979) Crystallographic studies of dynamic properties of lysozyme. Nature (London) 280:563–568

Austin RH, Beeson KW, Eisenstein L, Frauenfelder H, Gunsalus IC (1975) Dynamics of ligand binding to myoglobin. Biochemistry 14:5355–5373

Bartunik HD, Schubert P (1982) Crystal cooling for protein crystallography with synchrotron radiation. J Appl Cryst 15:227–231

Case DA, Karplus M (1979) Dynamics of ligand binding to heme proteins. J Mol Biol 132:343–368

Figgis BN, Reynolds PA, Lehner N (1983) cis-bis(bipyridy)dichloroiron(III) tetrachloroferrate(III), $[Fe(bpy)_2Cl_2][FeCl_4]$; structure at 4.2 and at 115 K by neutron diffraction. Acta Cryst B39:711–717

Frauenfelder H (1985) Ligand binding and protein dynamics. In: Clementi E, Corongiu G, Sarma MH, Sarma RH (eds), Structure and motions: membranes, nucleic acids and proteins. Adenine Press, pp 205–217

Frauenfelder H, Petsko GA, Tsernoglou D (1979), Temperature-dependent X-ray diffraction as a probe of protein structural dynamics. Nature 280:558–563

Frauenfelder H, Hartmann H, Karplus M, Kuntz ID, Kuriyan J, Parak F, Petsko GA, Ringe D, Tilton RF, Connolly MI, Max N (1987) The thermal expansion of a protein. Biochemistry 26:254–261

Hartmann H, Parak F, Steigemann W, Petsko GA, Ringe Ponzi D, Frauenfelder H (1982) Conformational substates in a protein; structure and dynamics of metmyoglobin at 80 K. Proc Natl Acad Sci USA 79:4967–4971

Hartmann H, Steigemann W, Reuscher H, Parak F (1986) Structural disorder in proteins: a comparison of myoglobin and erythrocruorin. Eur Biophys J 14: 337–348

Jones TA, Liljas L (1984) Crystallographic refinement of macromolecules having noncrystallographic symmetry. Acta Cryst A40:50–57

Kendrew JC, Parrish RG (1956) The crystal structure of myoglobin III. Sperm-whale myoglobin. Proc Roy Soc 238A: 305–324

Konnert JH (1976) A restrained parameter structure factor least-squares refinement procedure for large asymmetric units. Acta Crystallogr A32:614–617

Konnert JH, Hendrickson WA (1980) A restrained thermal factor refinement procedure. Acta Crystallogr A36:344–349

Krupyanskii Yu F, Parak F, Goldanskii VI, Mössbauer RL, Gaubmann F, Engelmann H, Suzdalev IP (1982) Investigation of large intramolecular movements within metmyoglobin by Rayleigh scattering of Mössbauer radiation (RSMR). Z. Naturforsch 37c:57–62

Levy RM, Sheridan RP, Keepers JW, Dubey GS, Swaminathan S, Karplus M (1985) Molecular dynamics of myoglobin at 298 K. Biophys J 48:509–518

Nienhaus GU, Parak F (1986) Rayleigh scattering of Mössbauer radiation on metmyoglobin. Hyperfine Interactions 29: 1451–1454

Nienhaus GU, Drepper F, Parak F, Mössbauer RL, Bade D, Hoppe W (1987) A multiwire proportional counter with spherical drift chamber for protein crystallography with X-rays and gamma-rays. Nucl Instrum Methods A256: 581–586

Nyborg J, Wonacott AJ (1977) In: Arnd UW, Wonacott AJ (eds) The rotation method in crystallography. North-Holland, Amsterdam, pp 139–145

Parak F, Knapp EW (1984) A consistent picture of protein dynamics. Proc Natl Acad Sci USA 81:7088–7092

Parak F, Thomanek UF, Bade D, Wintergerst B (1977) The orientation of the electric field gradient tensor in CO-liganded myoglobin. Z Naturforsch 32c:507–512

Parak F, Knapp EW, Kucheida D (1982) Protein dynamics. Mössbauer spectroscopy on deoxymyoglobin crystals. J Mol Biol 161:177–194

Parak F, Fischer M, Graffweg E, Formanek H (1987a) Distributions and fluctuations of protein structures investigated by X-ray analysis and Mössbauer spectroscopy. In: Clementi E, Chin S (eds) Structure and dynamics of nucleic acids, proteins and membranes. Plenum, New York, pp 139–148

Parak F, Hartmann H, Nienhaus GU, Heidemeier J (1987b) Structural fluctuations in myoglobin. In: Ehrenberg A, Rigler R, Gräslund A, Nilsson L (eds) Structure, dynamics and function of biomolecules. Springer, Berlin Heidelberg New York Tokyo, pp 30–33

Phillips SEV (1980)[1] Structure and refinement of oxymyoglobin at 1.6 A resolution. J Mol Biol 142:531–554

Reinisch L, Heidemeier J, Parak F (1985) Determination of the second order Doppler shift of iron in myoglobin by Mössbauer spectroscopy. Eur Biophys J 12:167–172

Ringe D, Petsko GA, Kerr DE, de Montellano PRO (1984) Reaction of myoglobin with phenylhydrazine: a molecular doorstop. Biochemistry 23:2–4

Schwager P, Bartels K (1975) Refinement of setting angles in screenless film methods. J Appl Crystallogr 8:275–280

Schwager P, Bartels K (1977) In: Arnd UW, Wonacott AJ (eds) The rotation method in crystallography. North-Holland, Amsterdam, pp 105–117, 139–151

Steigemann W (1974) Dissertation TU München. Die Entwicklung und Anwendung von Rechenverfahren und Rechenprogrammen zur Strukturanalyse von Proteinen am Beispiel des Trypsin-Trypsininhibitor-Komplexes, des freien Inhibitors und der L-Asparaginase

Swaminathan S, Craven BM, McMullan RK (1984) The crystal structure and molecular thermal motion of urea at 12, 60 and 123 K from neutron diffraction. Acta Crystallogr B40:300–306

Takano R (1977a)[1] Structure of myoglobin refined at 2.0 A resolution. Crystallographic refinement of metmyoglobin from sperm whale. J Mol Biol 110:537–568

Takano R (1977b)[1] Structure of myoglobin refined at 2.0 A resolution. Structure of deoxymyoglobin from sperm whale. J Mol Biol 110:569–584

[1] Coordinates taken from the Protein Data Bank